Commun Nonlinear Sci Numer Simulat 152 (2026) 109203

Contents lists available at ScienceDirect

Communications in Nonlinear Science and Numerical Simulation

journal homepage: www.elsevier.com/locate/cnsns

Research paper

An asymptotic solution for the planar Poiseuille flow of a power-law fluid with pressure-dependent wall slip

Lorenzo Fusi, Rebecca Tozzi *

Universitá degli Studi di Firenze, Dipartimento di Matematica e Informatica "Ulisse Dini", Viale Morgagni 67/A, 50134, Firenze, Italy

ARTICLE INFO

Keywords:
Planar Poiseuille flow
Power-law model
Pressure-dependent wall slip
Perturbation scheme

ABSTRACT

In this paper we study the plane Poiseuille flow of power-law fluids with pressure-dependent wall slip. In particular, we assume wall slip conditions which depend exponentially on pressure with a pressure-dependence slip decay parameter ε. The governing equations of the 2D, steady, symmetric flow are transformed into a system of nonlinear integro-differential equations with auxiliary (boundary, symmetry and integral) conditions. We use a regular perturbation scheme to obtain asymptotic solutions written as power series of ε, which is assumed to be a small parameter. We find approximate analytical solutions for all the components of both velocity field and pressure up to the first order. We investigate the behaviour of the longitudinal velocity, the slip velocity, the shear stress and the average pressure-drop for different values of the involved parameters. Our results show that the effects of pressure-dependent wall slip are more pronounced when wall slip is weak, while, for larger values of the slip coefficient, they are gradually eliminated. With regard to inertia, we show that the average pressure-drop remains constant untill the Reynolds number is sufficiently large.

1. Introduction

The "no-slip" boundary condition has been widely used in many studies concerning Newtonian and non-Newtonian flows (see for example Poole and Ridley [1], Richardson [2], Day [3], Lauga et al. [4]). It is a generally-accepted assumption in rheology, tribology and fluid mechanics [5]. However, the violation of this condition is broadly recognized in many situations, such as flow of polymer solutions, emulsions, yield stress fluids and suspensions, which exhibit wall slip at solid surfaces (see Barnes [6], Denn [7], Hatzikiriakos [8], Potente et al. [9], Mitsoulis et al. [10]). This observation led to a deeper investigation into the slip phenomenon, which had received little attention in early studies. Neto et al. [11] reviewed experimental studies on wall slip at solid interfaces, which are particularly relevant for microfluidic and microeletromechanical devices [12]. This phenomenon is especially important in the case of non-Newtonian fluids, where it is more pronounced and leads to interesting effects (see Sochi [5], Denn [7], Gryparis and Georgiou [13]). Sochi [5] noted that slip is more significant in non-Newtonian flows, as it affects the shear rate near the wall and, consequently, all parameters dependent on it [12]. Hatzikiriakos [8] examined both static and dynamic slip models in the context of rheology and flow simulations of molten polymers. In static slip models, the slip velocity u_w^* [1], defined as the relative velocity of adjacent fluid particles with respect to the wall, is assumed to be a function of the instantaneous wall shear stress τ_w^* [14]. Among the numerous models proposed in literature, one of the most common is the power-law model, in which the slip velocity is expressed

* Corresponding author.
E-mail address: rebecca.tozzi@unifi.it (R. Tozzi).

[1] Throughout the paper starred quantities represent dimensional variables.

https://doi.org/10.1016/j.cnsns.2025.109203
Received 9 May 2025; Received in revised form 23 July 2025; Accepted 5 August 2025
Available online 7 August 2025

as

$$u_w^* = \beta^* \tau_w^{*\,m}, \tag{1}$$

where β^* is the slip coefficient and m is the slip power-law exponent. The slip coefficient generally depends on temperature, normal stress, pressure, molecular parameters and the characteristics of the fluid-wall interface [12]. If $\beta^* = 0$, the no-slip condition is recovered, whereas for $m = 1$, Eq. (1) reduces to the classical Navier-slip condition. Experimental evidences suggest that the slip velocity may also depend on normal stresses (including pressure) and the history of local wall shear (see Hatzikiriakos [8] and references therein). In general, the slip coefficient (as well as the slip velocity) is a decreasing function of the normal stress. Hill et al. [15] proposed that the slip coefficient decays exponentially with the isotropic pressure p^*, leading to the following relation

$$u_w^* = A^* e^{-\varepsilon^*(p^* - p_{ref}^*)} \tau_w^*. \tag{2}$$

In (2), A^* is the slip coefficient at the reference pressure p_{ref}^* and ε^* is the pressure-dependence slip parameter. Other slip models have been proposed by Wang et al. [16], who considered temperature effects, as well as by Hatzikiriakos and Dealy [17], Tang and Kalyon [18,19], Tang [20], and Stewart [21], who suggested a density-dependent slip law. Damianou et al. [22] used (2) to investigate the steady, plane, axisymmetric and weakly compressible Poiseuille flow of a Herschel-Bulkley fluid, deriving approximate semi-analytical solutions. Panaseti et al. [12] Housiadas [23] applied a regular perturbation procedure to study Poiseuille flows of Newtonian and viscoelastic fluids, respectively, employing (2) as slip model. The study in Panaseti et al. [12] has been recently extended by Housiadas et al. [14], who analyzed the effect of wall slip in the form of (2) for Newtonian annular Poiseuille flow. They provided asymptotic solutions up to the second order in terms of the pressure decay parameter ε^*, which serves as a small perturbation parameter.

The aim of the present paper is to study the steady, symmetric, plane Poiseuille flow of power-law fluids with pressure-dependent wall slip, in order to extend our understanding of this type of slip phenomenon in different classes of fluids. The effects of other slip conditions in this geometry have already been investigated for Kountouriotis et al. [24], Ferrás et al. [25] and non-Newtonian fluids [26,27]. To our knowledge, this is the first study concerning power-law fluids with this specific type of wall slip conditions. The paper is organized as follows: in Section 2 we present the mathematical model and derive the governing equations in the form of nonlinear integro-differential equations combined with auxiliary conditions. In Section 3 we use the perturbation method (as in Housiadas et al. [14]) to obtain asymptotic solutions by assuming regular perturbation expansions in terms of ε, and we provide analytical solutions up to the first order. In Section 4 we show the results of the asymptotic analysis and we discuss the effect of pressure-dependent wall slip on the velocity and on the shear stress for different values of parameters such as slip coefficient, Reynolds number and slip decay. In Section 5 we summarize our main findings and conclusions.

2. The mathematical model

We investigate the steady, symmetric, planar Poiseuille flow of a power-law fluid in a straight channel of length L^* and width $2H^*$ under the assumption of pressure-dependent wall slip at rigid walls (see Fig. 1). More precisely, we consider an incompressible fluid described by the following constitutive equation

$$\mathbb{T}^* = -p^*\mathbb{I} + \mathbb{S}^*, \tag{3}$$

where

$$\mathbb{S}^* = 2\mu^*(\dot\gamma^*)\mathbb{D}^*, \quad \mu^*(\dot\gamma^*) = k^*(\dot\gamma^*)^{n-1}, \quad \dot\gamma^* = \sqrt{\frac{1}{2}\mathbb{D}^* \cdot \mathbb{D}^*}, \quad n > 0. \tag{4}$$

In (3) and (4), $-p^*\mathbb{I}$ is the indeterminate part of the stress due to the constraint of incompressibility, $\mathbb{S}^*$ is the deviatoric part of the stress, $\mathbb{D}^*$ is the symmetric part of the velocity gradient (i.e., the rate-of-deformation tensor). The apparent viscosity $\mu^*(\dot\gamma^*)$ is assumed

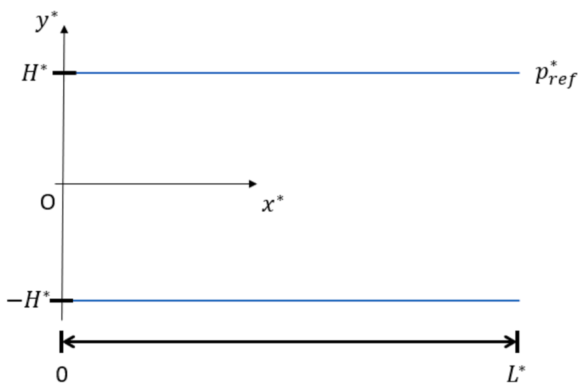

Fig. 1. Geometry of the problem.

to be a function of $\dot{\gamma}^*$, the Frobenius norm of $\mathbb{D}^*$. Here, k^* denotes the consistency index and n is the flow behaviour index. The flow is assumed to be two-dimensional and steady, with a velocity field of the following form

$$\mathbf{v}^* = u^*(x^*, y^*)\,\mathbf{e}_x + v^*(x^*, y^*)\,\mathbf{e}_y,$$

where y^* is the transversal coordinate and x^* represents the distance from the inlet point (see Fig. 1). Because of symmetry we require that the velocity $\mathbf{v}^*$ is an even function of y^*.

In the absence of volume forces, the equations governing the flow are the balance of mass and the balance of linear momentum, namely

$$\begin{cases} \mathrm{div}(\mathbf{v}^*) = 0, \\ \rho^*\left(\nabla\mathbf{v}^*\right)\mathbf{v}^* = -\nabla p^* + \mathrm{div}(\mathbb{S}^*), \end{cases}$$

where ρ^* is the constant mass density of the fluid. The boundary conditions at the rigid plates are pressure-dependent wall slip and no-penetration. Specifically, we assume that the longitudinal velocity on $y^* = \pm H^*$ is proportional to the shear stress through a function which decays exponentially with pressure and that the transversal velocity vanishes, that is

$$u^* = -\mathrm{sgn}(y^*)A^* e^{-\varepsilon^*(p^*-p^*_{ref})} S^*_{12}, \quad v^* = 0 \quad \text{at } y^* = \pm H^*, \tag{5}$$

where A^* is the constant slip coefficient, p^*_{ref} is a reference pressure and ε^* is the pressure-dependence slip parameter. The latter is assumed to be small and has the dimensions of the inverse of a pressure. We suppose that the volumetric flow rate Q^* at the inlet cross-section and the outlet pressure at the upper right corner of the channel wall are prescribed:

$$\int_{-H^*}^{H^*} u^*(0, y^*)\,dy^* = Q^*, \quad p^*(L^*, H^*) = p^*_{ref}. \tag{6}$$

We rescale the variables as

$$x^* = L^* x, \qquad y^* = H^* y, \qquad u^* = U^*_m u, \qquad \delta = \frac{H^*}{L^*}, \qquad v^* = \left(\delta U^*_m\right) v,$$
$$p^* = P^*_c p + p^*_{ref}, \qquad \dot{\gamma}^* = \left(\frac{U^*_m}{H^*}\right)\dot{\gamma}, \qquad \mathbb{D}^* = \left(\frac{U^*_m}{H^*}\right)\mathbb{D}, \qquad \mathbb{S}^* = \left(\mu^*_0 \frac{U^*_m}{H^*}\right)\mathbb{S}, \qquad \mu^*(\dot{\gamma}^*) = \mu^*_0 \mu(\dot{\gamma}),$$
$$\varepsilon^* = \left(\frac{1}{P^*_c}\right)\varepsilon,$$

where

$$\mu^*_0 := k^*\left(\frac{U^*_m}{H^*}\right)^{n-1}, \quad \mathbb{S} = 2\mu(\dot{\gamma})\mathbb{D}, \quad \mu(\dot{\gamma}) = \dot{\gamma}^{n-1},$$
$$U^*_m = \frac{Q^*}{2H^*} = \frac{1}{2H^*}\int_{-H^*}^{H^*} u^*(0, y^*)\,dy^* \tag{7}$$

with U^*_m mean velocity and P^*_c characteristic pressure, that has to be specified.
Selecting

$$P^*_c = \frac{k^* U^{*n}_m L^*}{H^{*n+1}},$$

we get the following non-dimensional expressions for the rate-of-deformation and stress tensors

$$\mathbb{D} = \frac{1}{2}\begin{pmatrix} 2\delta u_x & u_y + \delta^2 v_x \\ u_y + \delta^2 v_x & 2\delta v_y \end{pmatrix}, \quad \mathbb{S} = \dot{\gamma}^{n-1}\begin{pmatrix} 2\delta u_x & u_y + \delta^2 v_x \\ u_y + \delta^2 v_x & 2\delta v_y \end{pmatrix}$$

respectively, where

$$\dot{\gamma} = \sqrt{\delta^2 u_x^2 + \frac{1}{4}(u_y + \delta^2 v_x)^2}. \tag{8}$$

We define the Reynolds number as

$$\mathrm{Re} = \frac{\rho^* U^*_m H^*}{\mu^*_0} = \frac{\rho^* U^{*\,2-n}_m H^{*n}}{k^*}.$$

The non-dimensional governing equations become

$$\begin{cases} u_x + v_y = 0, \\ \mathrm{Re}\delta(u_x u + u_y v) = -p_x + \delta(S_{11})_x + (S_{12})_y, \\ \mathrm{Re}\delta^3(v_x u + v_y v) = -p_y + \delta^2(S_{12})_x + \delta(S_{22})_y. \end{cases} \tag{9}$$

The boundary conditions (5) and (6) become

$$u = -\mathrm{sgn}(y)Ae^{-\varepsilon p}u_y\left(\delta^2 u_x^2 + \frac{1}{4}u_y^2\right)^{\frac{n-1}{2}}, \quad v = 0 \quad \text{at } y = \pm 1, \tag{10}$$

$$p(1,1)=0, \tag{11}$$

where $A := (A^*k^*U_m^{*n-1})/H^{*n}$ is the dimensionless slip number and ε is the dimensionless pressure-dependence slip decay parameter. We note that, due to the continuity equation and the no-penetration conditions, the flow rate is constant at any cross-section of the channel. In the non-dimensional formulation we find

$$\int_{-1}^{1} u(x,y)\,dy = 2.$$

Furthermore, since the longitudinal velocity u is required to be an even function of y, we focus on the half plane $y>0$ and use the following set of the auxiliary (boundary, symmetry and integral) conditions for $y\in[0,1]$:

$$\begin{cases} u = -Ae^{-\varepsilon p}u_y\left(\delta^2 u_x^2 + \dfrac{1}{4}u_y^2\right)^{\frac{n-1}{2}} \quad \text{at } y=1,\\ u_y = 0 \quad \text{at } y=0,\\ v=0 \quad \text{at } y=0,1,\\ \displaystyle\int_0^1 u(x,y)\,dy = 1,\\ p(1,1)=0. \end{cases} \tag{12}$$

Our problem thus consists of (9) combined with (12). We observe that if $A=0$, the well-known no-slip condition is recovered, with both velocity components vanishing on the plates. If $\varepsilon=0$, then the slip velocity u on the walls no longer depends on pressure p and, consequently, (10) reduces to the classical Navier-slip condition, wherein the longitudinal velocity is independent of x and is a function only of y. The balance of linear momentum along the x-direction can be rewritten in conservative form, as shown in Housiadas et al. [14]. Skipping all the algebraic manipulations for which we refer the reader to Housiadas et al. [14], we obtain the following expression for the longitudinal velocity u

$$\begin{aligned} u(x,y) = \mu^{-1}(x,y)\Bigg\{ & u(x,1)\left[\mu(x,1) + \frac{e^{\varepsilon p(x,1)}}{A}(1-y)\right] + \mathrm{Re}\delta\left[-\int_y^1 u(x,z)v(x,z)\,dz + \frac{\partial}{\partial x}\int_y^1\int_{\tilde y}^1 u^2(x,z)\,dz\,d\tilde y\right] \\ & + \frac{\partial}{\partial x}\int_y^1\int_{\tilde y}^1 p(x,z)\,dz\,d\tilde y - \int_y^1 u(x,z)\frac{\partial}{\partial z}\mu(x,z)\,dz + \delta^2\int_y^1 \mu(x,z)\frac{\partial}{\partial x}v(x,z)\,dz - 2\delta^2\frac{\partial}{\partial x}\int_y^1\int_{\tilde y}^1 \mu(x,z)\frac{\partial}{\partial x}u(x,z)\,dz\,d\tilde y\Bigg\}. \end{aligned} \tag{13}$$

The total force balance along the main flow direction is given by

$$\mathrm{Re}\delta\,\frac{\partial}{\partial x}\int_0^1 u^2(x,y)\,dy + \frac{\partial}{\partial x}\int_0^1 p(x,y)\,dy + \frac{u(x,1)}{A}e^{\varepsilon p(x,1)} - 2\delta^2\frac{\partial}{\partial x}\int_0^1 \mu(x,y)\frac{\partial}{\partial x}u(x,y)\,dy = 0. \tag{14}$$

Expressions (13) and (14) have been derived using $(9)_1$, $(12)_1$, $(12)_2$, $(12)_3$.
In conclusion, Eqs. $(9)_1$, (13), $(9)_3$ constitute a system of nonlinear integro-differential equations for the unknowns u, v, p that cannot be solved explicitly. We will obtain an approximate solution by treating ε as a small perturbation parameter and performing an asymptotic analysis up to the first order.

3. Perturbation solution in terms of ε

Due to symmetry, we restrict our analysis to the upper half of the channel, defined by

$$\{(x,y)|0\le x\le 1,\ 0\le y\le 1\}.$$

Following Housiadas et al. [14], we express the solution as a regular perturbation expansion in terms of ε, which is assumed to be a small parameter. In particular, for $\varepsilon=0$ (that is the case of Navier-slip condition), the flow is fully developed: the transversal velocity vanishes, the longitudinal velocity depends only on the transversal coordinate and the pressure gradient is constant throughout the flow domain. Following Housiadas et al. [14], we look for a solution written as power series of ε in the following way

$$\begin{aligned} u &= \underbrace{u^{(0)}(y)}_{u_0} + \varepsilon\underbrace{\left(u^{(10)}(y) + \hat x u^{(11)}(y)\right)}_{u_1} + O(\varepsilon^2),\\ v &= \varepsilon\underbrace{v^{(1)}(y)}_{v_1} + O(\varepsilon^2),\\ p &= \underbrace{p^{(0)}\hat x}_{p_0} + \varepsilon\underbrace{\left(p^{(10)}(y) + \hat x p^{(11)} + \hat x^2 p^{(12)}\right)}_{p_1} + O(\varepsilon^2),\\ w &= \underbrace{w^{(0)}}_{w_0} + \varepsilon\underbrace{\left(w^{(10)} + \hat x w^{(11)}\right)}_{w_1} + O(\varepsilon^2), \end{aligned} \tag{15}$$

where we set

$$\hat{x} := 1 - x, \quad w(\hat{x}) := u(\hat{x}, 1).$$

For simplicity, we have introduced the new variable $\hat{x}$ and we have handled the longitudinal velocity on the upper plate as a separate unknown variable. In the present analysis, we shall consider the zero and first order solutions.

3.1. Zero-order solutions

At the leading order, using (15), (13), (12), we find

$$u^{(0)}(y)\left(-\frac{u_y^{(0)}(y)}{2}\right)^{n-1} = w^{(0)}\left(t^{(0)}(1) + \frac{1-y}{A}\right) - p^{(0)}\left(\frac{1}{2} - y + \frac{y^2}{2}\right) - \int_y^1 u^{(0)}(z)\frac{\partial}{\partial z}t^{(0)}(z)\,dz, \tag{16}$$

where

$$t^{(0)}(y) := \left(-\frac{u_y^{(0)}(y)}{2}\right)^{n-1}, \quad \frac{\partial}{\partial y}t^{(0)}(y) = -\frac{n-1}{2}\left(-\frac{u_y^{(0)}(y)}{2}\right)^{n-2} u_{yy}^{(0)}(y),$$

combined with the auxiliary conditions

$$\begin{aligned} & w^{(0)} + Au_y^{(0)}(1)\left(-\frac{u_y^{(0)}(1)}{2}\right)^{n-1} = 0, \\ & u_y^{(0)}(0) = 0, \\ & \int_0^1 u^{(0)}(y)\,dy = 1. \end{aligned} \tag{17}$$

From (14), we get that $w^{(0)} = Ap^{(0)}$. Therefore, inserting the expression of $w^{(0)}$ in (16) and using (17), we end up with the following formulas for the leading-order solutions in the interval $[0, 1]$:

$$u_0 = u^{(0)}(y) = Ap^{(0)} + \left(2^{n-1}p^{(0)}\right)^{\frac{1}{n}}\frac{n}{n+1}\left(1 - y^{\frac{n+1}{n}}\right), \tag{18}$$

$$p_0 = p^{(0)}\hat{x} = p^{(0)}(1-x), \tag{19}$$

$$w_0 = w^{(0)} = Ap^{(0)}. \tag{20}$$

All the variables are expressed in terms of the zero-order pressure difference $p^{(0)}$ which has to satisfy Eq. (21)

$$Ap^{(0)} + \left(2^{n-1}p^{(0)}\right)^{\frac{1}{n}}\frac{n}{2n+1} = 1, \tag{21}$$

that admits a unique solution, as shown in Fig. 2.

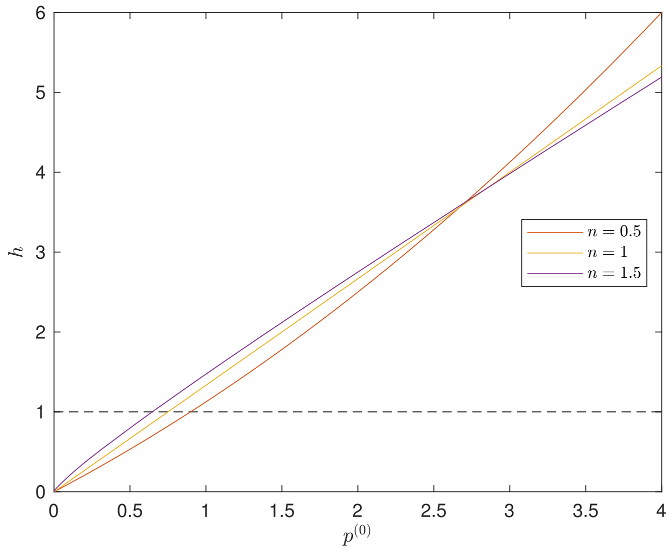

Fig. 2. Plot of the function $h(p^{(0)}) = Ap^{(0)} + (2^{n-1}p^{(0)})^{\frac{1}{n}}\frac{n}{2n+1}$ and of the solutions of the Eq. (21) $h(p^{(0)}) = 1$ for different values of $n = 0.5,\ 1,\ 1.5$.

3.2. First-order solutions

Mass balance $(9)_1$ at first-order and $(12)_2$ allows one to get an expression for $v^{(1)}(y)$ in terms of $u^{(11)}(y)$, that is

$$v^{(1)}(y) = -\int_y^1 u^{(11)}(z)\,dz. \tag{22}$$

Exploiting $(9)_3$ and (14), we write the three components of the first-order pressure as

$$p^{(10)}(y) = \delta^2 \int_y^1 \left(-\frac{u_z^{(0)}(z)}{2}\right)^{n-2} \left[\frac{2-n}{2} u_z^{(11)}(z) u_z^{(0)}(z) + (n-1) u_{zz}^{(0)}(z) u^{(11)}(z)\right] dz, \tag{23}$$

$$p^{(11)} = -2\mathrm{Re}\delta \int_0^1 u^{(0)}(y) u^{(11)}(y)\; dy + \frac{w^{(10)}}{A}, \tag{24}$$

$$p^{(12)} = \frac{w^{(11)}}{2A} + \frac{p^{(0)2}}{2}. \tag{25}$$

Then, considering (13) at $O(\varepsilon)$ and using (22), (24), (25), (18), (16) and (12), the first-order perturbation problem has the following form for the unknowns $u^{(10)}(y)$, $u^{(11)}(y)$:

$$\begin{aligned}
u^{(10)}(y) = &-\left(-\frac{u_y^{(0)}(y)}{2}\right)^{-2} \frac{n-1}{4} u_y^{(0)}(y) u_y^{(10)}(y) u^{(0)}(y) + \left(-\frac{u_y^{(0)}(y)}{2}\right)^{-n+1} \Bigg\{ w^{(10)}\left[t^{(0)}(1) + \frac{1-y^2}{2A}\right] \\
&+ \frac{n-1}{4} w^{(0)} \left(-\frac{u_y^{(0)}(1)}{2}\right)^{n-3} u_y^{(0)}(1) u_y^{(10)}(1) + \mathrm{Re}\delta\Bigg[\int_y^1 u^{(0)}(\tilde{y}) \int_{\tilde{y}}^1 u^{(11)}(z)\,dz\,d\tilde{y} \\
&- 2\int_y^1 \int_{\tilde{y}}^1 u^{(0)}(z) u^{(11)}(z)\,dz\,d\tilde{y} + \left(1-2y+y^2\right) \int_0^1 u^{(0)}(y) u^{(11)}(y)\; dy\Bigg] \\
&- \int_y^1 u^{(10)}(z) \frac{\partial}{\partial z} t^{(0)}(z)\,dz - \frac{n-1}{4} \int_y^1 u^{(0)}(z) \left(-\frac{u_z^{(0)}(z)}{2}\right)^{n-3} \left[(n-2) u_{zz}^{(0)}(z) u_z^{(10)}(z) + u_z^{(0)}(z) u_{zz}^{(10)}(z)\right] dz \Bigg\},
\end{aligned} \tag{26}$$

$$\begin{aligned}
u^{(11)}(y) = &-\left(\frac{u_y^{(0)}(y)}{2}\right)^{-2} \frac{n-1}{4} u_y^{(0)}(y) u_y^{(11)}(y) u^{(0)}(y) + \left(-\frac{u_y^{(0)}(y)}{2}\right)^{-n+1} \Bigg\{ w^{(11)}\left[t^{(0)}(1) + \frac{1-y^2}{2A}\right] \\
&+ \frac{n-1}{4} w^{(0)} \left(-\frac{u_y^{(0)}(1)}{2}\right)^{n-3} u_y^{(0)}(1) u_y^{(11)}(1) + p^{(0)2} \frac{1-y^2}{2} - \int_y^1 u^{(11)}(z) \frac{\partial}{\partial z} t^{(0)}(z)\,dz \\
&- \frac{n-1}{4} \int_y^1 u^{(0)}(z) \left(-\frac{u_z^{(0)}(z)}{2}\right)^{n-3} \left[(n-2) u_{zz}^{(0)}(z) u_z^{(11)}(z) + u_z^{(0)}(z) u_{zz}^{(11)}(z)\right] dz \Bigg\},
\end{aligned} \tag{27}$$

completed with the following conditions

$$\begin{gathered}
w^{(10)} + nA u_y^{(10)}(1) \left(-\frac{u_y^{(0)}(1)}{2}\right)^{n-1} = 0, \quad w^{(11)} + A\left(-\frac{u_y^{(0)}(1)}{2}\right)^{n-1} \left(-p^{(0)} u_y^{(0)}(1) + n u_y^{(11)}(1)\right) = 0, \\
u_y^{(10)}(0) = 0, \quad u_y^{(11)}(0) = 0, \int_0^1 u^{(10)}(y)\,dy = 0, \quad \int_0^1 u^{(11)}(y)\,dy = 0.
\end{gathered} \tag{28}$$

The expressions of the transversal velocity and the three components of pressure can be determined once $u^{(10)}$, $u^{(11)}$ are found, thanks to (22)–(25).

We observe that, if we consider the solutions we have found (i.e., (18)–(27)) with $n = 1$, they are equivalent to those presented in Panaseti et al. [12], Housiadas et al. [14], taking into account the differences in the coordinate systems used.

3.3. Analytical resolution

It is worth noting that Eq. (27) is decoupled from Eq. (26); thus, we can first focus on the solution $u^{(11)}(y)$, and substitute it into the equation for $u^{(10)}(y)$ at a later time.

To simplify the notation, we set

$$f(y) := u^{(10)}(y), \quad g(y) := u^{(11)}(y), \quad G := p^{(0)}. \tag{29}$$

Then, using (29) and (18), (20) to explicitly calculate the various coefficients in (27) and (28), after several algebraic manipulations (that are too lengthy to be reported here but can be provided upon requested), we get the following linear boundary value problem for $g(y)$ on the interval $[0,1]$

$$\begin{cases} g'(y)n + \left(\frac{G}{2}\right)^{\frac{1}{n}-1} y^{\frac{1}{n}} \left(\frac{\gamma}{A} + G^2\right) = 0, \\ g'(0) = 0, \\ g'(1) = -\frac{1}{n}\left(\frac{G}{2}\right)^{\frac{1}{n}-1}\left(\frac{\gamma}{A} + G^2\right). \end{cases} \tag{30}$$

In (30) $\gamma := g(1)$ plays the role of a parameter. In other words, the solution of (30) is of the form $g(y;\gamma)$, and γ must be selected so that the integral condition in (28)

$$\int_0^1 g(y;\gamma)\, dy = 0, \tag{31}$$

is satisfied. Integrating $(30)_1$ between y and 1, we get

$$g(y) = \gamma + \frac{1}{n+1}\left(\frac{G}{2}\right)^{\frac{1}{n}-1}\left(\frac{\gamma}{A} + G^2\right)\left(1 - y^{\frac{n+1}{n}}\right). \tag{32}$$

Inserting (32) in (31), we find

$$\gamma = -\left[1 + \frac{1}{A(2n+1)}\left(\frac{G}{2}\right)^{\frac{1}{n}-1}\right]^{-1} \frac{1}{2n+1}\left(\frac{G}{2}\right)^{\frac{1}{n}-1} G^2. \tag{33}$$

Now we use the same procedure for $f(y)$ and we solve the following problem

$$\begin{cases} f'(y)n + \frac{\theta}{A}\left(\frac{G}{2}\right)^{\frac{1}{n}-1} y^{\frac{1}{n}} - \mathrm{Re}\delta\left(\frac{G}{2}\right)^{\frac{1}{n}-1}\left\{ y^{\frac{1}{n}}\left[\frac{AG\gamma n}{n+1} + \gamma\left(\frac{G}{2}\right)^{\frac{1}{n}} \frac{2n^3(4n+3)}{(n+1)^2(3n+2)(2n+1)}\right]\right. \\ \left. + y^{\frac{n+2}{n}}\left[-\frac{AG\gamma n}{n+1} - \gamma\left(\frac{G}{2}\right)^{\frac{1}{n}} \frac{4n^3}{(n+1)^2(2n+1)}\right] + y^{\frac{2n+3}{n}}\left[\gamma\left(\frac{G}{2}\right)^{\frac{1}{n}} \frac{2n^3}{(n+1)^2(3n+2)}\right]\right\} = 0, \\ f'(0) = 0, \\ f'(1) = -\frac{\theta}{nA}\left(\frac{G}{2}\right)^{\frac{1}{n}-1}, \end{cases} \tag{34}$$

which is again a linear boundary value problem in $[0,1]$ for the unknown $f(y;\theta)$, where $\theta := f(1)$ must be chosen in such a way that

$$\int_0^1 f(y;\theta)\, dy = 0. \tag{35}$$

Proceeding as before, we obtain the following formula for $f(y)$:

$$\begin{aligned} f(y) = \theta &+ \frac{\theta}{A(n+1)}\left(\frac{G}{2}\right)^{\frac{1}{n}-1}\left(1 - y^{\frac{n+1}{n}}\right) - \mathrm{Re}\delta\left(\frac{G}{2}\right)^{\frac{1}{n}-1}\left\{\left[\frac{AG\gamma n}{n+1} + \gamma\left(\frac{G}{2}\right)^{\frac{1}{n}} \frac{2n^3(4n+3)}{(n+1)^2(3n+2)(2n+1)}\right]\right. \\ &\frac{1}{n+1}\left(1 - y^{\frac{n+1}{n}}\right) - \left[\frac{AG\gamma n}{n+1} + \gamma\left(\frac{G}{2}\right)^{\frac{1}{n}} \frac{4n^3}{(n+1)^2(2n+1)}\right]\frac{1}{2(n+1)}\left(1 - y^{\frac{2n+2}{n}}\right) \\ &\left. + \left[\gamma\left(\frac{G}{2}\right)^{\frac{1}{n}} \frac{2n^3}{(n+1)^2(3n+2)}\right]\frac{1}{3(n+1)}\left(1 - y^{\frac{3n+3}{n}}\right)\right\}, \end{aligned} \tag{36}$$

with θ being

$$\theta = \left[\left(\frac{G}{2}\right)^{1-\frac{1}{n}} + \frac{1}{A(2n+1)}\right]^{-1} \mathrm{Re}\delta\left(\frac{G}{2}\right)^{\frac{1}{n}-1}\left\{\left[\frac{AG\gamma n}{n+1} + \gamma\left(\frac{G}{2}\right)^{\frac{1}{n}} \frac{2n^3(4n+3)}{(n+1)^2(3n+2)(2n+1)}\right]\right. \tag{37}$$

$$\left.\frac{1}{2n+1} - \left[\frac{AG\gamma n}{n+1} + \gamma\left(\frac{G}{2}\right)^{\frac{1}{n}} \frac{4n^3}{(n+1)^2(2n+1)}\right]\frac{1}{3n+2} + \left[\gamma\left(\frac{G}{2}\right)^{\frac{1}{n}} \frac{2n^3}{(n+1)^2(3n+2)}\right]\frac{1}{4n+3}\right\}. \tag{38}$$

4. Results

In this section we show some plots to illustrate the behaviour of the longitudinal velocity, the slip velocity, the shear stress and the average pressure-drop along the channel for different values of the involved parameters. In particular, we consider three values of the flow behaviour index n, namely $n = 0.5,\ 1,\ 1.5$, to analyze the differences between shear-thinning, Newtonian and shear-thickening behaviours. Each plot below refers to the upper part of the channel $[0,1]$ (profiles are symmetric in the negative half-plane $[-1,0]$).

We start investigating the ranges of the dimensionless parameters for which the perturbation solutions remain valid. Since the exponential $e^{-\varepsilon p}$ is positive, its first-order series expansion should also remain positive. Thus, we look for the ranges of (A,ε) such that

$$e^{-\varepsilon p} \approx 1 - \varepsilon p_0 > 0,$$

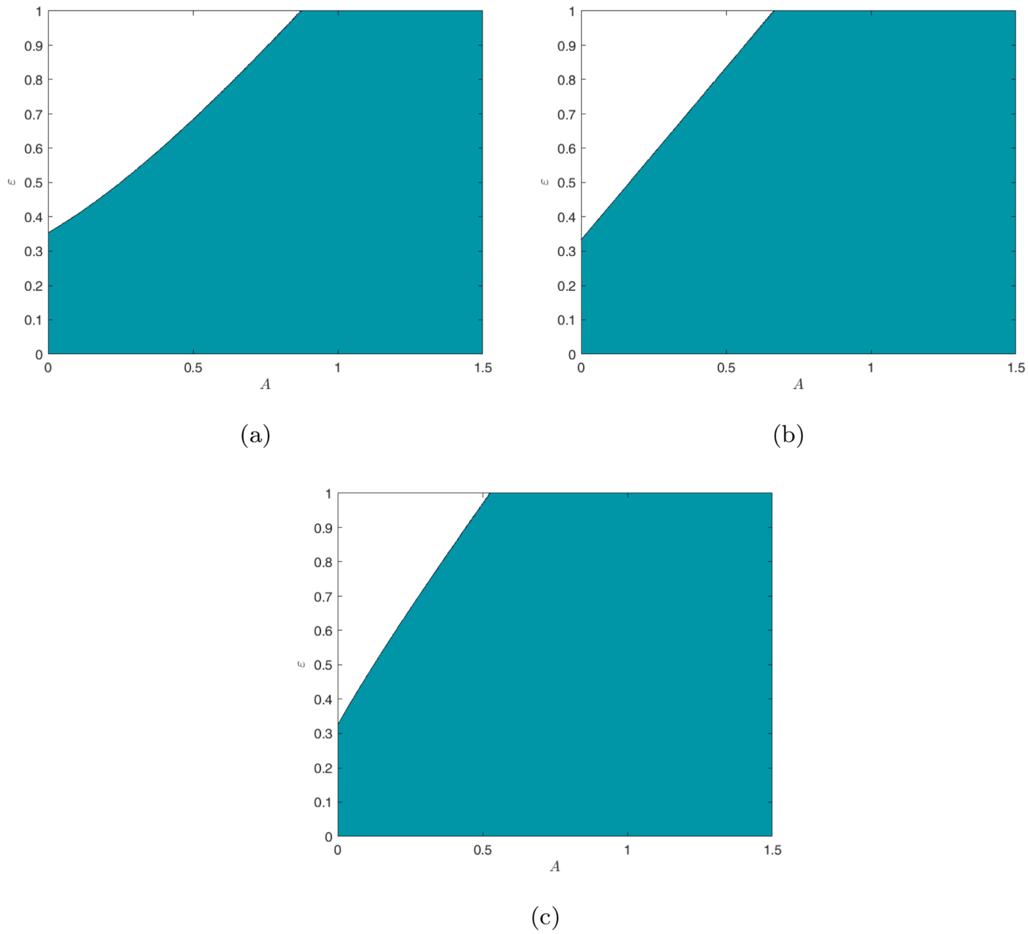

Fig. 3. Plot of the admissible range (shaded area) of the parameters ε and A for which $e^{-\varepsilon p} > 0$ for any values of the x-coordinate with Re $= 1$, $\delta = 1$ for (a) $n = 0.5$, (b) $n = 1$, (c) $n = 1.5$.

for all values of the x-coordinate, where p_0 can be considered as a function of A. In Fig. 3 the green area represents the admissible values of (A, ε) which guarantee the positivity of the exponential series expansion for every x and for $n = 0.5$, 1, 1.5, Re $= 1$ and $\delta = 1$. We note that the lower the slip coefficient A is, the smaller the slip decay parameter ε has to be. Conversely, moving away from the no-slip case $A = 0$, larger values of ε are allowed (but $\varepsilon < 1$). Moreover, the admissible range of the dimensionless parameters (A, ε) increases as n increases.

As mentioned in Section 3, the zero-order solution $u_0(y)$ corresponds to the fully developed plane Poiseuille velocity with Navier-slip conditions at the walls. In this case, u_0 does not depend on x, the transversal velocity is zero, and the pressure varies linearly with x. At first order, we have pressure-dependent wall slip conditions, and the longitudinal velocity becomes a function of x

$$u(x, y) = u_0(y) + \varepsilon u_1(x, y),$$

while the transversal velocity $v = v^{(1)}(y)$ is no longer zero. In Fig. 4 we display the deviation of the velocity profile bewteen first and zero order, that is $\delta u(x, y) = u(x, y) - u_0(y) = \varepsilon u_1(x, y)$, as a function of y for selected downstream distances $x = 0.1$, 0.5, 0.9 and for $n = 0.5$, 1, 1.5. The other parameters are $A = 1$, Re $= 1$, $\delta = 1$, $\varepsilon = 0.5$. In Fig. 5 we show the longitudinal velocity contours $u(x, y) = u_0(y) + \varepsilon u_1(x, y)$ for $n = 0.5$, 1, 1.5 (with $A = 1$, Re $= 1$, $\delta = 1$, $\varepsilon = 0.5$). For every value of n, the velocity is higher in the central part of the channel and decreases towards the wall. In particular, near the wall, it increases with x, whereas near the centerline $y = 0$ it exhibits opposite behaviour. With regard to the dependence on n, we observe that u increases globally with n meaning that in the shear-thickening case the longitudinal velocity varies much more than in the shear-thinning case. In particular, when $n > 1$, the fluid is more viscous, and its velocity has to be larger since a constant volumetric flow rate is imposed. Fig. 6 shows the plot of the slip velocity $w(x)$ for $n = 0.5$, 1, 1.5 and $\varepsilon = 0.01$, 0.2, 0.5 (with $A = 1$, Re $= 1$, $\delta = 1$). We note that increasing ε leads to a decrease in the slip velocity, and that $w(x)$ is a decreasing function of the flow behaviour index n. Regarding the shear stress, at first order it is given by

$$S_{12} \approx -2^{1-n}\left(-\frac{\partial u_0}{\partial y}\right)^n + \varepsilon\, n 2^{1-n}\left(-\frac{\partial u_0}{\partial y}\right)^{n-1}\frac{\partial u_1}{\partial y}. \tag{39}$$

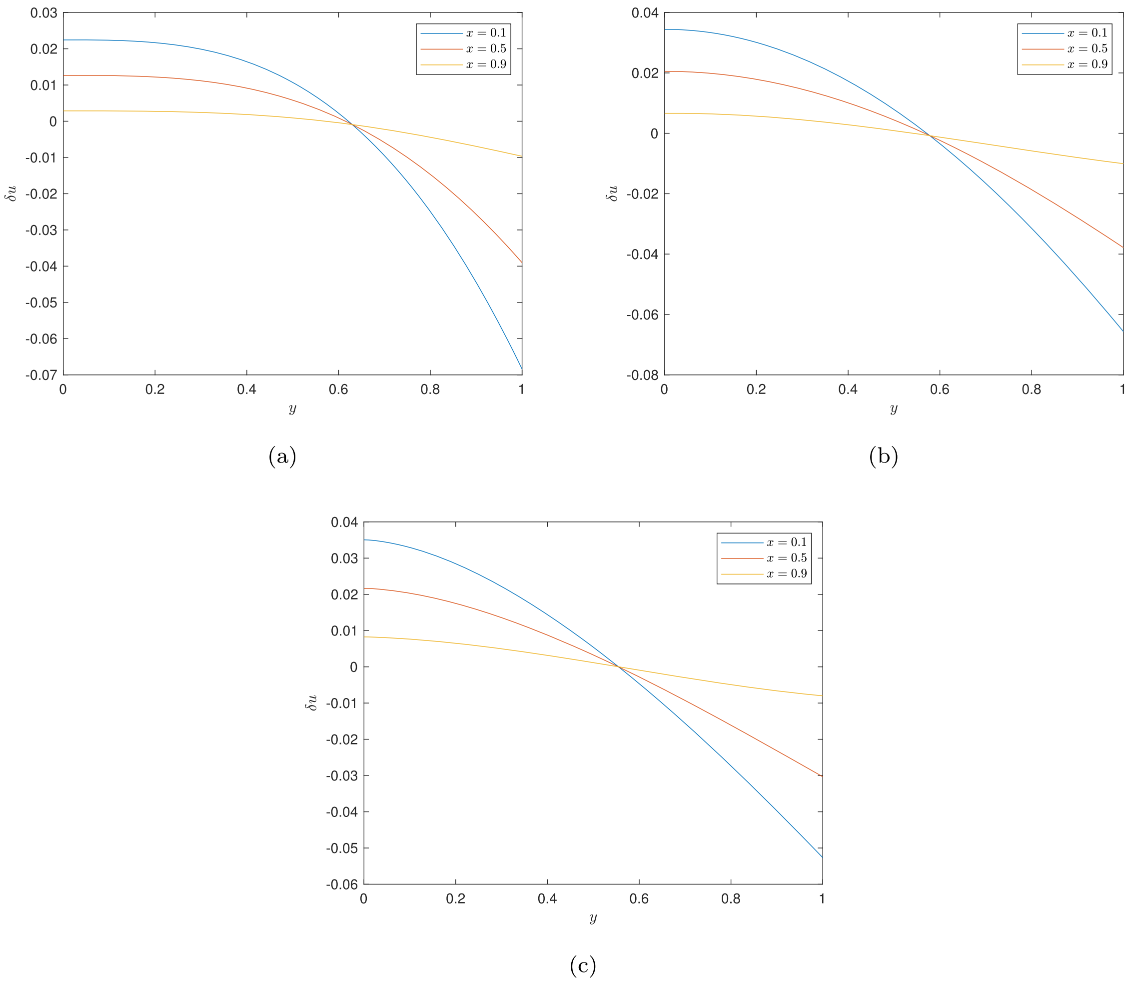

Fig. 4. Plot of the devation of the velocity profile $\delta u = \varepsilon u_1(x, y)$ as a function of y with $A = 1$, Re $= 1$, $\delta = 1$, $\varepsilon = 0.5$, for selected downstream distances $x = 0.1, 0.5, 0.9$ and for (a) $n = 0.5$, (b) $n = 1$, (c) $n = 1.5$.

In Fig. 7 we display the shear stress contours for (a) $n = 0.5$, $\varepsilon = 0.01$, (b) $n = 0.5$, $\varepsilon = 0.5$, (c) $n = 1$, $\varepsilon = 0.01$, (d) $n = 1$, $\varepsilon = 0.5$, (e) $n = 1.5$, $\varepsilon = 0.01$, (f) $n = 1.5$, $\varepsilon = 0.5$ (with $A = 1$, Re $= 1$, $\delta = 1$). First, we observe that the dependence on x is negligible for "very" small values of ε. We also notice that, in each plot, the shear stress increases (in modulus) towards the rigid wall, consistent with our earlier observations on the velocity. In proximity of the wall, the dependence of S_{12} on the longitudinal coordinate x is much more pronounced than in the inner regions of the channel. In addition, the absolute value of the shear stress decreases as the flow behaviour index increases, meaning that it grows moving from shear-thickening to shear-thinning fluids due to the increased dissipation.

Finally, we investigate the average pressure-drop along the channel, $\Delta < p >$, which plays an important role in designing and optimizing fluid flow systems such as pipelines, ventilation systems and chemical reactors (see Housiadas et al. [14]). Since pressure p depends on both x and y, we consider the difference of the average pressures between the inlet and the outlet plane, defined as

$$\Delta < p > := 2\int_0^1 p(0, y) - p(1, y)\, dy, \tag{40}$$

where $\Delta f := f(x = 0, y) - f(x = 1, y)$ for any function $f = f(x, y)$. In our case, an alternative formula for $\Delta < p >$ can be derived from the total force balance by integrating (14) with respect to x from 0 and 1, yielding

$$\Delta < p > = -2\mathrm{Re}\delta\Delta\left[\int_0^1 u^2(x, y)\, dy\right] + 4\delta^2\Delta\left[\int_0^1 \mu(x, y)\frac{\partial}{\partial x}u(x, y)\, dy\right] + 2\int_0^1 \frac{w(x)}{A}e^{\varepsilon p(x,1)}\, dx. \tag{41}$$

Thus, the average pressure-drop is composed of three components: the difference in kinetic energy between the inlet and the outlet cross-sections of the channel, a viscous contribution due to the nonlinearity of the power-law model and the kinetic energy transferred along the walls due to slip (which is always positive due to the positivity of the slip velocity). Inserting (15) in (40), (41) and expanding up to the first order, we find

$$\Delta < p > \approx \Delta < p_0 > + \varepsilon\Delta < p_1 >,$$

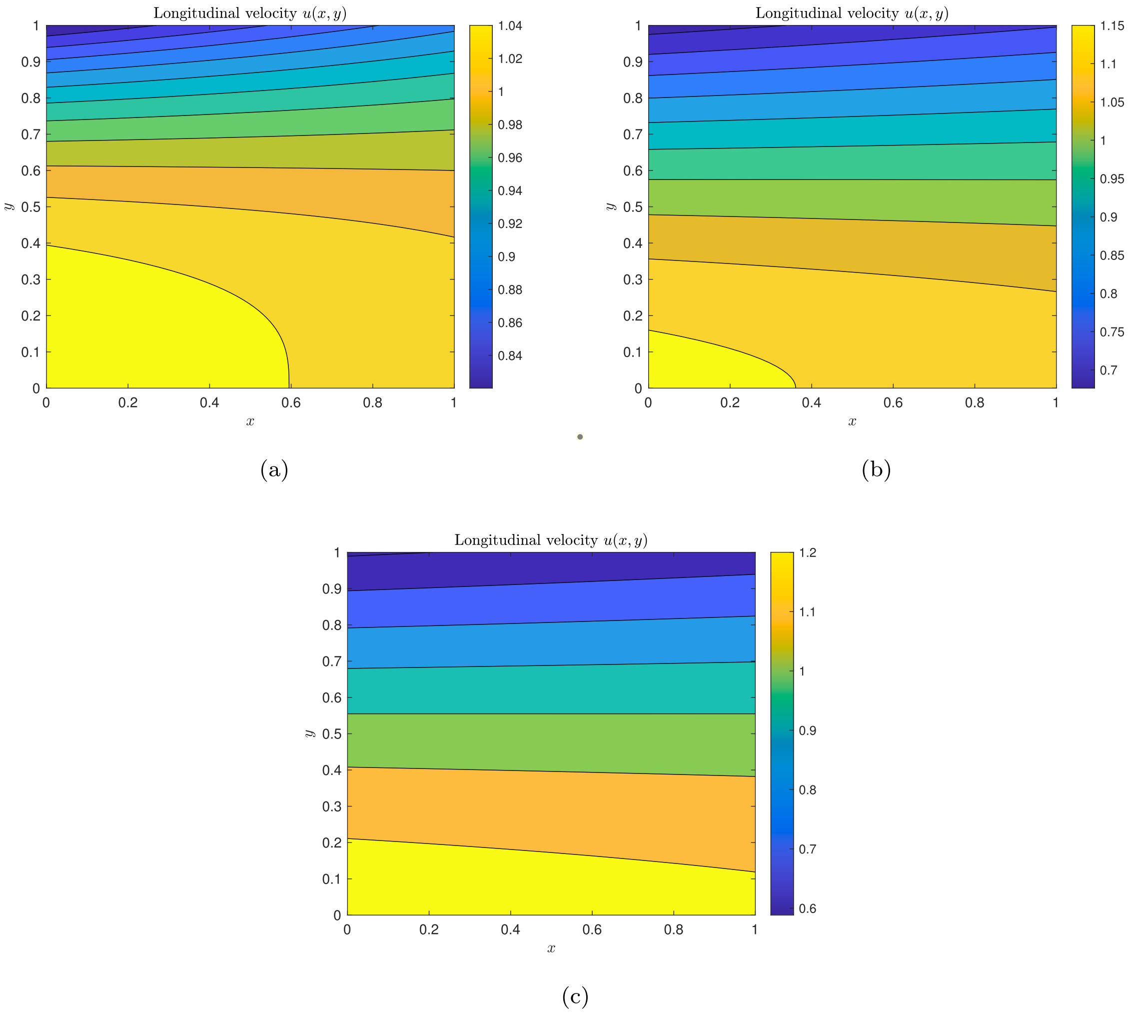

Fig. 5. Longitudinal velocity contours $u(x,y)$ with $A=1$, $\mathrm{Re}=1$, $\delta=1$, $\varepsilon=0.5$ for (a) $n=0.5$, (b) $n=1$, (c) $n=1.5$.

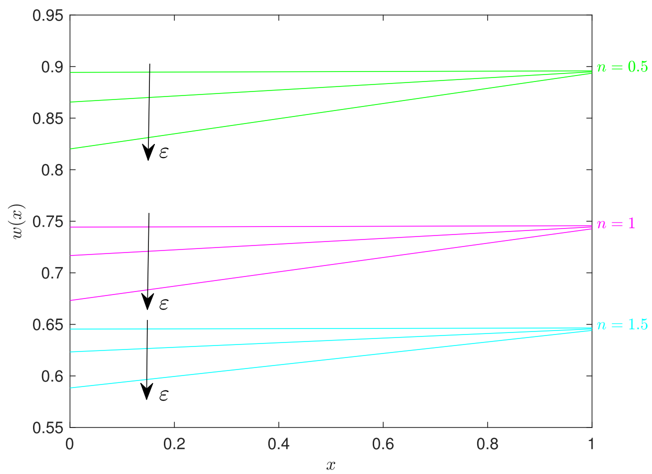

Fig. 6. Plot of the slip velocity $w(x)$ with $A=1$, $\mathrm{Re}=1$, $\delta=1$ for $n=0.5$, 1, 1.5 and $\varepsilon=0.01$, 0.2, 0.5.

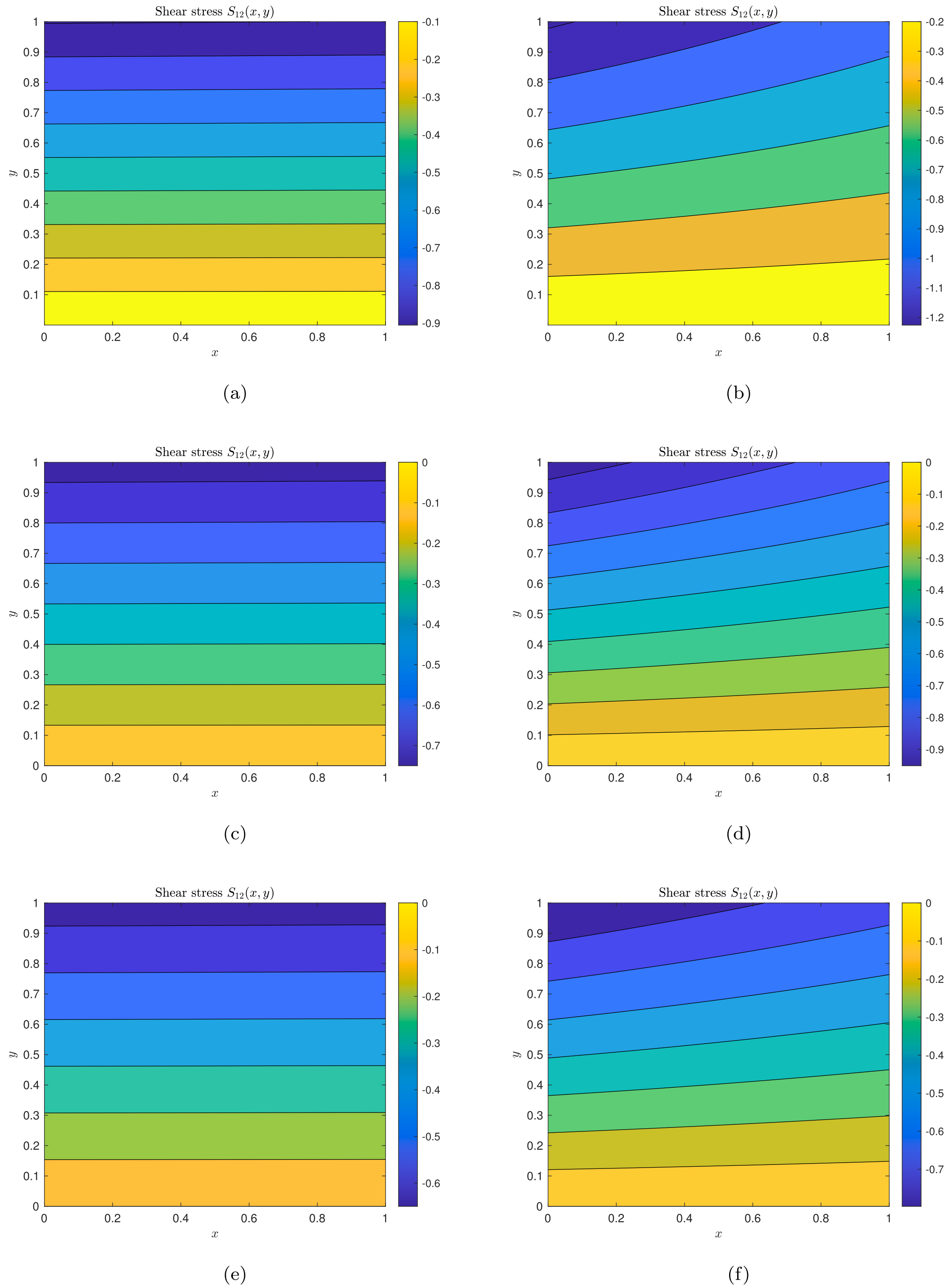

Fig. 7. Shear stress contours $S_{12}(x, y)$ at the first order with $A = 1$, Re $= 1$, $\delta = 1$ for (a) $n = 0.5$, $\varepsilon = 0.01$, (b) $n = 0.5$, $\varepsilon = 0.5$, (c) $n = 1$, $\varepsilon = 0.01$, (d) $n = 1$, $\varepsilon = 0.5$, (e) $n = 1.5$, $\varepsilon = 0.01$, (f) $n = 1.5$, $\varepsilon = 0.5$.

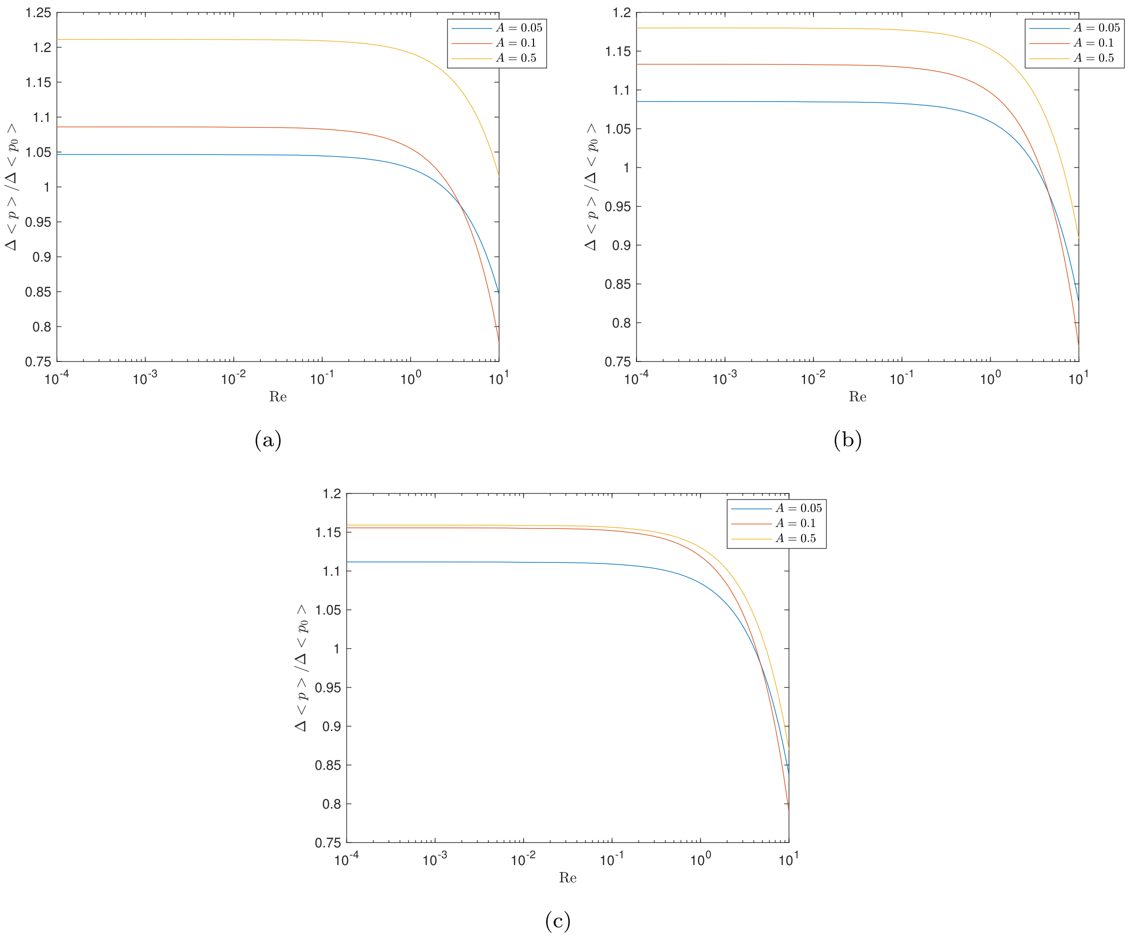

Fig. 8. Plot of the reduced average pressure-drop $\Delta < p > /\Delta < p_0 >$ as a function of Re with $A = 0.05$, 0.1, 0.5, $\delta = 1$, $\varepsilon = 0.5$ for (a) $n = 0.5$, (b) $n = 1$, (c) $n = 1.5$.

where

$$\Delta < p_0 > = \frac{2w^{(0)}}{A},$$

$$\Delta < p_1 > = -4\mathrm{Re}\delta \int_0^1 u^{(0)}(y)u^{(11)}(y)\,dy + \frac{2}{A}\left(w^{(10)} + \frac{w^{(11)}}{2}\right) + \frac{(\Delta < p_0 >)^2}{4}.$$

In Figs. 8 and 9 we present plots of the reduced average pressure-drop $\Delta < p > /\Delta < p_0 >$ in terms of Re with $A = 0.05$, 0.1, 0.5 and as a function of A with Re $= 0$, 5, respectively. In both cases, we consider $n = 0.5$, 1, 1.5 (with fixed $\delta = 1$, $\varepsilon = 0.5$). Regarding the dependence on the Reynolds number, we find that the pressure drop remains constant untill Re is sufficiently large, and then it decreases monotonically. Looking at $\Delta < p > /\Delta < p_0 >$ as a function of the slip coefficient (with Re $= 0$) (see the blue line in Fig. 9), we observe that, for values of A “very” close to 0 (i.e., no-slip condition), the pressure-drop increases sharply with A due to the variation of the slip velocity along the channel (as shown in Fig. 5). Then, for larger values of A, the required pressure-drop decreases smoothly without steep gradients. Instead, when Re $= 5$ (see the red line in Fig. 9), $\Delta < p > /\Delta < p_0 >$ first decreases rapidly near the origin and then it follows the same behaviour of before. The effect of inertia is that of a slight reduction of the average pressure-drop for small and moderate slip parameters, while for larger A this effect decreases more and more. In particular, the impact of pressure-dependent slip conditions is more pronounced for smaller values of n, i.e., for shear-thinning fluids. More precisely, as the flow behaviour index increases, that is moving from shear-thinning ($n < 1$) to shear-thickening fluids ($n > 1$), the slip velocity decreases in magnitude (see Fig. 6) and, consequently, the effect of pressure diminishes. In addition, we notice that the smaller the flow behaviour index n is, the sooner the plots corresponding to the two different Reynolds number tend to coincide, indicating that the effect of inertia fades more quickly.

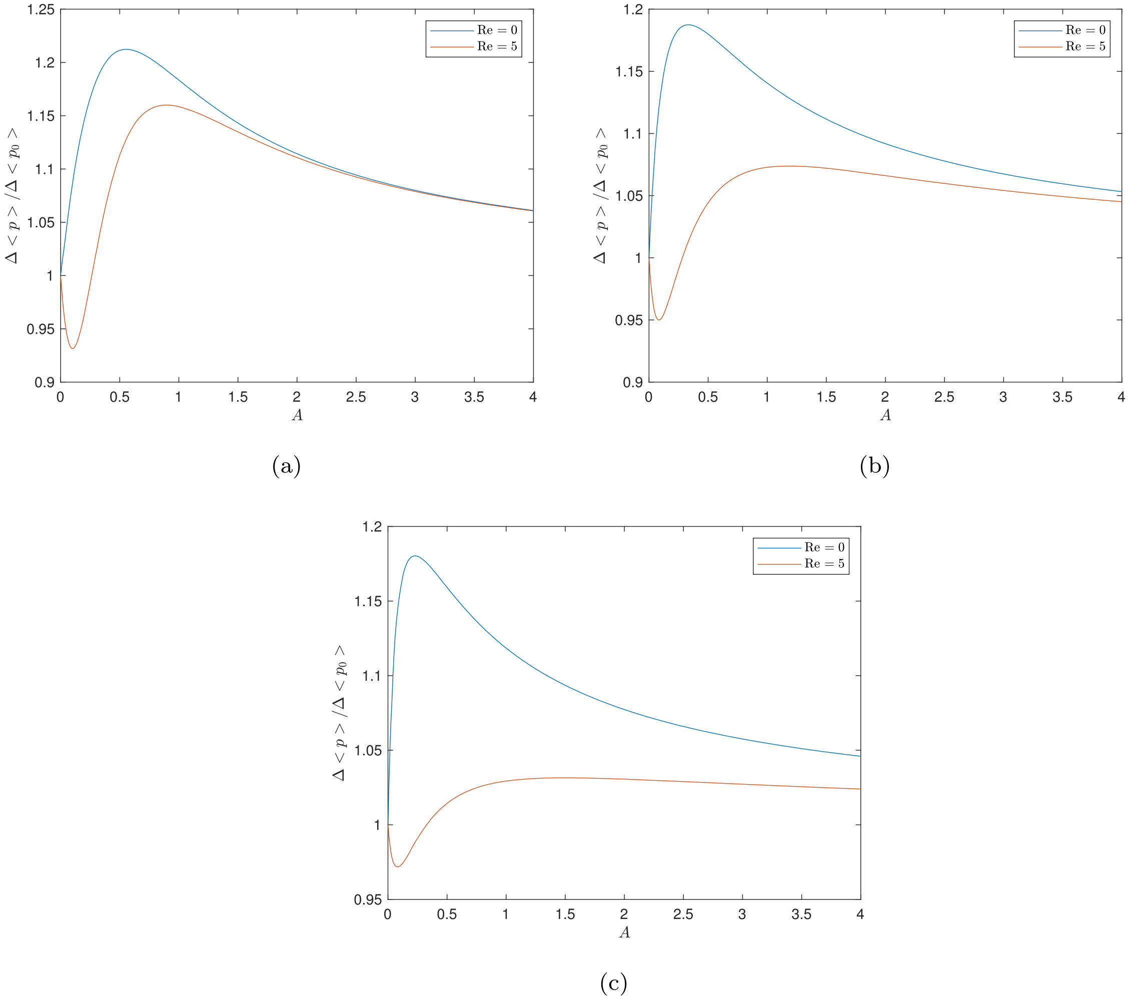

Fig. 9. Plot of the reduced average pressure-drop $\Delta < p > /\Delta < p_0 >$ as a function of A with Re $= 0, 5$, $\delta = 1$, $\epsilon = 0.5$ for (a) $n = 0.5$, (b) $n = 1$, (c) $n = 1.5$.

5. Conclusions

We have investigated the plane Poiseuille flow of power-law fluids with pressure-dependent wall slip. In particular, we have assumed wall slip conditions which depend exponentially on pressure with a small pressure-dependence slip decay coefficient ϵ. The dimensionless governing equations for the 2D, steady, symmetric, planar flow have been transformed into a system of nonlinear integro-differential equations with boundary, symmetry and integral conditions, where the unknowns are the components of the velocity field and pressure. We have looked for solutions in the form of regular perturbation expansions (as in Housiadas et al. [14]) in terms of ϵ which is assumed to be a small perturbation parameter. Approximate analytical solutions up to first order have been provided for all the involved variables. We have analyzed the behaviour of the longitudinal velocity, the slip velocity, the shear stress and the average pressure-drop for different values of the physical parameters, including the flow behaviour index n. We have found that the longitudinal velocity reaches its maximum near the inlet section close to the centerline of the channel. Moreover, the longitudinal velocity decreases with x near the axis $y = 0$ and increases with x in the vicinity of the solid wall. The slip velocity is found to be a decreasing function of both the pressure-dependent slip coefficient and the flow behaviour index. The modulus of the shear stress increases with y (opposite to the behaviour of the longitudinal velocity) and decreases with n. Finally, we have studied the behaviour of the average pressure-drop as a function of the Reynolds number and the slip parameter. Our findings show that the effect of pressure on slip gradually fades as slip increases and, irrespective of n, the slip velocity tends to a constant value along the channel. In particular, the impact of pressure-dependent slip conditions is more pronounced for shear-thinning fluids than for shear-thickening fluids. More precisely, as the flow behaviour index increases, i.e., moving from $n < 1$ to $n > 1$, the slip velocity decreases in magnitude and, consequently, so does the effect of pressure. With regard to inertia, we have provided that sufficiently large Reynolds numbers produce a decrease in the pressure-drop.

One possible development of the present work could be the application of this method to other geometrical settings or to fluids described by implicit constitutive relations.

CRediT authorship contribution statement

Lorenzo Fusi: Methodology, Formal analysis, Investigation, Writing – original draft, Writing – review & editing; **Rebecca Tozzi:** Methodology, Formal analysis, Investigation, Writing – original draft, Writing – review & editing.

Data availability

No data was used for the research described in the article.

Declaration of interests

The authors declare that they have no known competing financial interests or personal relationships that could have appeared to influence the work reported in this paper.

Acknowledgements

The present work has been performed under the auspices of the Italian National Group for Mathematical Physics (GNFM-Indam). This work has been done under the framework PRIN 2022 project "Mathematical modelling of heterogeneous systems" financed by the European Union - Next Generation EU, CUP B53D23009360006/B53D23009370006, Project Code 2022MKB7MM, PNRR M4.C2.1.1.

References

[1] Poole RJ, Ridley BS. Development-length requirements for fully developed laminar pipe flow of inelastic non-Newtonian liquids 2007.
[2] Richardson S. On the no-slip boundary condition. J Fluid Mech 1973;59(4):707–19.
[3] Day MA. The no-slip condition of fluid dynamics. Erkenntnis 1990;33(3):285–96.
[4] Lauga E, Brenner MP, Stone HA. Microfluidics: the no-slip boundary condition. arXiv preprint arXiv:cond-mat/0501557 2005.
[5] Sochi T. Slip at fluid-solid interface. Polym Rev 2011;51(4):309–40.
[6] Barnes HA. A review of the slip (wall depletion) of polymer solutions, emulsions and particle suspensions in viscometers: its cause, character, and cure. J Non-Newton Fluid Mech 1995;56(3):221–51.
[7] Denn MM. Extrusion instabilities and wall slip. Annu Rev Fluid Mech 2001;33(1):265–87.
[8] Hatzikiriakos SG. Wall slip of molten polymers. Prog Polym Sci 2012;37(4):624–43.
[9] Potente H, Ridder H, Cunha RV. Global concept for describing and investigation of wall slip effects in the extrusion process. Macromol Mater Eng 2002;287(11):836–42.
[10] Mitsoulis E, Kazatchkov IB, Hatzikiriakos SG. The effect of slip in the flow of a branched PP melt: experiments and simulations. Rheol Acta 2005;44:418–26.
[11] Neto C, Evans DR, Bonaccurso E, Butt H-J, Craig V SJ. Boundary slip in Newtonian liquids: a review of experimental studies. Rep Prog Phys 2005;68(12):2859.
[12] Panaseti P, Housiadas KD, Georgiou GC. Newtonian Poiseuille flows with pressure-dependent wall slip. J Rheol 2013;57(1):315–32.
[13] Gryparis E, Georgiou GC. Torsional parallel plate flow of Herschel-Bulkley fluids with wall slip. Phys Fluid 2024;36(4).
[14] Housiadas KD, Gryparis E, Georgiou GC. Annular Newtonian Poiseuille flow with pressure-dependent wall slip. Eur J Mech-B/Fluid 2025;109:299–308.
[15] Hill DA, Hasegawa T, Denn MM. On the apparent relation between adhesive failure and melt fracture. J Rheol 1990;34(6):891–918.
[16] Wang ZY, Lam YC, Chen X, Joshi SC. Viscosity corrections for concentrated suspension in capillary flow with wall slip. AlChE J 2010;56(6):1447–55.
[17] Hatzikiriakos SG, Dealy JM. Wall slip of molten high density polyethylenes. II. Capillary rheometer studies. J Rheol 1992;36(4):703–41.
[18] Tang HS, Kalyon DM. Unsteady circular tube flow of compressible polymeric liquids subject to pressure-dependent wall slip. J Rheol 2008;52(2):507–25.
[19] Tang HS, Kalyon DM. Time-dependent tube flow of compressible suspensions subject to pressure dependent wall slip: ramifications on development of flow instabilities. J Rheol 2008;52(5):1069–90.
[20] Tang H. Analysis on creeping channel flows of compressible fluids subject to wall slip. Rheol Acta 2012;51:421–39.
[21] Stewart CW. Wall slip in the extrusion of linear polyolefins. J Rheol 1993;37(3):499–513.
[22] Damianou Y, Georgiou GC, Moulitsas I. Combined effects of compressibility and slip in flows of a Herschel-Bulkley fluid. J Non-Newton Fluid Mech 2013;193:89–102.
[23] Housiadas KD. Viscoelastic Poiseuille flows with total normal stress dependent, nonlinear Navier slip at the wall. Phys Fluid 2013;25(4).
[24] Kountouriotis Z, Philippou M, Georgiou GC. Development lengths in Newtonian Poiseuille flows with wall slip. Appl Math Comput 2016;291:98–114.
[25] Ferrás LL, Afonso AM, Alves MA, Nóbrega JM, Pinho FT. Development length in planar channel flows of Newtonian fluids under the influence of wall slip 2012.
[26] Ferrás LL, Nóbrega JM, Pinho FT. Analytical solutions for Newtonian and inelastic non-Newtonian flows with wall slip. J Non-Newton Fluid Mech 2012;175:76–88.
[27] Frigaard IA, Howison SD, Sobey IJ. On the stability of Poiseuille flow of a Bingham fluid. J Fluid Mech 1994;263:133–50.